# EXPERIMENTAL STUDY ON HYDROGEN/AIR PREMIXED FLAME PROPAGATION IN CLOSED RECTANGULAR CHANNELS

**Shen, X.[1], Zhang, C.[1], Wen, J.X.[2], Xiu, G.[1]**
**[1] School of Resources & Environmental Engineering, East China University of Science and Technology, Meilong Road, Shanghai, 200237, PR China, ustcshenxb@gmail.com**
**[2] Warwick FIRE, School of Engineering, University of Warwick**
**Coventry, CV4 7AL, UK, Jennifer.Wen@warwick.ac.uk**

## ABSTRACT

Hydrogen combustion and explosion in confined spaces, e.g. chambers, channels, corridors, pipelines, or underground galleries, are of great concerns and importance in hydrogen safety. To fully understand the flame regimes and underlying mechanisms in relevant accidental phenomena, present study observed the evolutions during flame propagation of hydrogen/air premixed flame in two channels with different aspect ratios which simulate the confined spaces. The schlieren system and the pressure sensor were used to capture flame shapes and pressure changes in the channels. It was found that the different aspect ratios resulted in distinct flame shape evolutions and dynamics. Larger acceleration rate and more drastic fluctuations of both flame tip velocity and pressure were recorded in the channel with larger aspect ratio. Some interesting flame shapes such as the "T-shaped flame", the second flat flame and the second tulip flame were found in the channel with larger aspect ratio. The experimental data in the channel with larger width coincided better with Bychkov's analytical theory. The results also suggested that the pressure wave is not the major cause of tulip flame formation, but it is an important factor during the further flame shape evolution after the classic inversion. Instead, the flame deceleration after flame touching the wall was regarded as the primary cause.

## 1.0 INTRODUCTION

Fossil fuel has long been a major source of energy. With the large development of industry and the increasing needs from human beings, the fossil fuel will be exhausted soon in the future. In addition, fossil fuel has caused a series of environmental issues, e.g. greenhouse effect. Thus, it necessitates the demand of environmentally friendly alternative fuel. Hydrogen is widely regarded as one of the most promising clean energy carrier [1, 2]. However, hydrogen has wide flammability range, high diffusivity, very low ignition energy and large burning velocity, which makes it a great hazard in industry. Therefore, safety is of great importance in hydrogen production, storage, transportation and utilization. Especially in confined spaces, once hydrogen was exposed to air or other oxidizers, combustible mixtures would be readily formed and then accidentally ignited by energy source. The subsequent flame propagation and transition (from laminar to turbulence, or from deflagration to detonation) are quite complex. In worst cases, the flame is able to produce violent pressure and temperature rise, and even strong shock waves, which could probably lead to serious fatalities and destructions. Therefore, for safe use of hydrogen, it is necessary to gain insight of its combustion and flame propagation processes in confined spaces. Usually the structures of channels (tubes) were used to simulate the confined spaces in the laboratory.

The pioneering work of premixed flame in channels was reported by Mallard and Le Chatelier [3] in 1883, in which a special flame structure was firstly detected. Ellis [4] took the first photograph of the inverted flame in the channel in 1928. Salamandra [5] et al. named this featured flame shape as "tulip flame". Thereafter, Clanet and Searby [6] distinguished four characteristic stages of tulip flame formation in channels, including spherical flame expansion, finger-shaped flame acceleration, flame-side wall contact and the tulip inversion.

Considerable amount of investigations have been carried out to get insight of this interesting flame phenomena, leading to discussions about the effects of wall quenching, squish flow, flame and pressure wave interaction, and flame instabilities. For instance, Markstein [7] experimentally observed that the interaction between the flame and the shock wave with the latter pushed the unburned gas rapidly into the burned gas, resulting in the Taylor instability. He suggested that the shock wave would facilitate the inversion of the flame. On the contrary, Starke and Roth [8] gave a different explanation. They used the tracer particles to measure the shape and velocity of the flame and attributed the flame inversion to the deceleration of the flame which was caused by the

reduction of the flame area after the flame-side wall contact. Pocheau and Kwon [9] triggered two paratactic ignitions simultaneously in one channel, and observed the formation of two adjacent tulip flames without boundary layer between them, which implied the possibility of boundary layer being of minimum effects. Xiao et al. [10] proposed that the inversion of the flame front and the formation of the tulip flame are due to the interactions among the flame front, the flame-induced reverse flow and the vortices. The reverse flow and vortices cause the velocities in the near wall region to be higher than that of the middle section, forming tulip flame.

However, in the experiments of Dunn-Rankin and Sawyer [11], they investigated many factors which can influence the formation of the tulip flame and its behavior and concluded that the basic tulip flame is a robust phenomenon, which mainly depends on the overall geometry of the combustion vessel while the other factors have minimum effects. For the later period of flame propagation, Xiao et al. [12] demonstrated the possibility of a new stage, namely the "distorted tulip flame". In this stage, an outstanding tulip distortion can be formed after full tulip formation in the equivalence ratio range between 0.84 and 4.22 in closed channel. In this phenomenon, two inversions occur on the two flame lips after the classic tulip flame forms.

The scale effect was also found to have great influence on flame propagation [13]. Chen and Guo [14] found that the growth rate of velocity and pressure changed in closed channels with different aspect ratios. Yu et al. [15] conducted the experiments in venting channels and concluded that the aspect ratio influenced the formation of tulip flames. Xiao et al. [16] took successive frames of flame fronts from calculations of different aspect ratios and sizes and found that the flame accelerated faster, the pressure waves were stronger and the flame structures were more wrinkled in channels with larger aspect ratio. However, more investigations are required to characterize the influence of aspect ratio on the flame structure and dynamics. Therefore, present study focused on the aspect ratio effect on flame propagation in closed channels with aspect ratios of 6.625 and 12, respectively.

## 2.0 EXPERIMENTAL

The experiments were conducted in two horizontal rectangular combustion channels with different aspect ratios. The test rig is equipped with a schlieren system, a high-speed camera, a gas mixing system, a high-voltage ignition, a pressure recording system, a synchronization controller and a data acquisition system. The channels have two quartz visible sidewalls for schlieren photography. The top and bottom walls are TP304 stainless steel.

The dimensions of the two channels are channel (a) 300 mm × 25 mm × 25 mm and channel (b) 530 mm × 80 mm × 80 mm, giving aspect ratios "α", i.e. length over width, of 12 and 6.625. The experiments in channel (b) has been done in our previous work [17]; but the data are cited here and re-analysed for deeper understanding of flame behaviors.

The hydrogen and air were mixed in the gas mixing system before they were injected into the channel. After a few minutes' standing in the channel, the hydrogen-air mixture was ignited by a high-voltage igniter with a spark gap on the axis of the channel near the left end wall. The subsequent evolution of the flame shape was recorded by the high-speed schlieren imaging system. The pressure sensors were placed at the top wall collecting the pressure dynamics. The synchronization controller coordinated the start-ups of the entire devices.

The experiments were performed at initial conditions of 298 K and 101325 Pa. The gas purity was 99.999% for hydrogen and 99.95% for air. The equivalence ratios of the mixtures are set around 1.

## 3.0 RESULTS AND DISCUSSION

### 3.1 Flame shape changes

The premixed flames of hydrogen-air mixture in present two channels both underwent the classic flame deformation in the early four stages as divided by Clanet and Searby [6]. A time series of flame images in the channel with α=12 are shown in Fig.1. The first stage (0 ms < t < 0.4 ms) started shortly after the ignition. In this stage, flame appeared at the axis near the left end wall and expanded as a spherical shape. It was unaffected by the boundary. After the characteristic time $t_{sphere}$=0.4 ms, the flame approached the sidewall and was stretched into a finger shape due to the confinement of the sidewall. This process was defined as the second stage (0.4 ms < t < 1.2 ms).

The flame surface area grew rapidly during this interval. At t=1.2 ms, the flame skirt arrived at the sidewall. This was followed by the third stage (1.2 ms < t < 2.4 ms) during which the flame skirt touched the sidewall and the contact point moved along the wall chasing the flame front on the centerline. At t =2.4 ms, the flame front became planar, which was followed immediately by the inversion of the flame front, i.e. the flame front on the centerline propagated backwards forming a cusp. The flame front close to the walls turned to the leading tips. The distance between the cusp and the flame tips increased drastically, forming a deep "tulip flame" shape. After the four classic stages, a "T-shaped flame" was observed for the first time at around t=4 ms in present experiments. The cusp collapsed to a line with two tulip flame lips very close to each other. At the meantime, the flame front became flat once again with a gap at the center presenting a "T" shape consequently. At t=4.2 ms, the "T-shaped flame" broke down and the front of the flame tended to be curved. At about t=6 ms, a second classic tulip flame appeared and underwent a distorted tulip deformation. The subsequent combustion process was similar to those discussed in our previous studies [16-19].

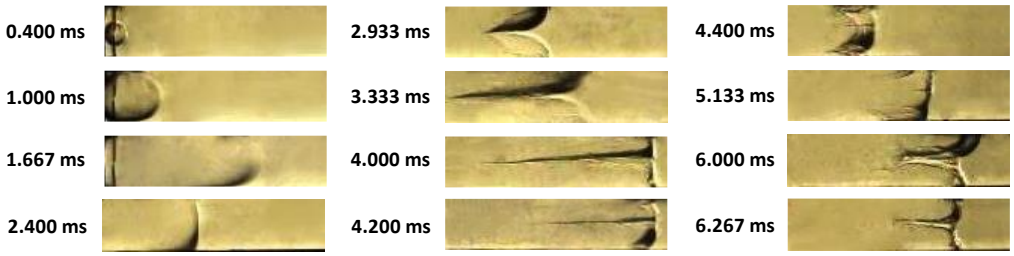


Figure 1. Flame shape changes in channel (a) with α=12

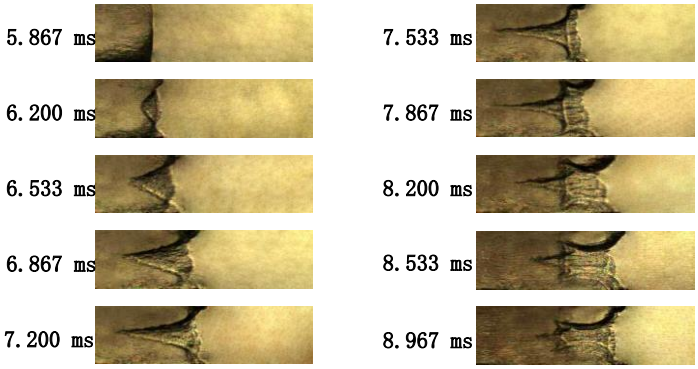


Figure 2. Flame shape changes in channel (b) with α=6.625

For flame shape changes in the channel (b) shown in Fig.2, a tulip flame was formed with the same process as that in channel (a). The flat flame front appeared at t=5.867 ms which was later than the time in channel (a). The measured distances between the flame central point and the front side differed significantly in the two channels. The tulip flame in channel (a) was much more elongated like a "T-shaped flame" while a classic tulip flame was seen in channel (b). In the later stages, the flame shape in channel (a) became more complex, changing from the "T-shaped flame" to the curved flame, then the second flat front flame appeared. This was followed by the second tulip flame and finally the distorted tulip flame. In channel (b), the flame shape directly changed to distorted tulip flame after the formation of the classic tulip flame.

### 3.2 Flame and pressure dynamics

The propagation velocity of the flame tip versus time in channel (a) is showed in Fig.3. The flame tip in the context is defined as the cutting edge of the flame front. It can be seen that the velocity fluctuated periodically with time. At about t=1.6 ms, the velocity reached its maximum value. In this acceleration process, the flame was in a finger-shaped structure. The flame front was stretched due to the constrain of the sidewall and the flame surface area increased sharply, which is regarded as the main reason for the flame acceleration. When the flame front touched the sidewall, the wall-quenching effect resulted in the rapid reduction of the flame surface area accompanied by the reduced acceleration of the flame front. At approximately t=2.334 ms, the flame tip velocity became zero while the flame turned planar. Then a cusp in the opposite direction of the flame propagation was generated and the tulip flame was formed. After the formation of the classic tulip

flame, the cusp was suddenly elongated from t=3.067 ms with a remarkable increase of the flame surface area. At the meantime, the flame velocity underwent an abrupt increase. After the tulip flame was elongated, the two tulip flame lips began to coalesce. At t=3.867 ms, the flame structure transformed to "T" shape. The flame tip velocity reached its minimal value when the "T-shaped flame" happened, but the flame front area did not decrease. Following this, the flame lips coalesced thoroughly, and the flame shape changed to a second curving front pointing to the unburned gas and the velocity increased again. This was followed by the second flat flame, second tulip flame and the distorted tulip flame.

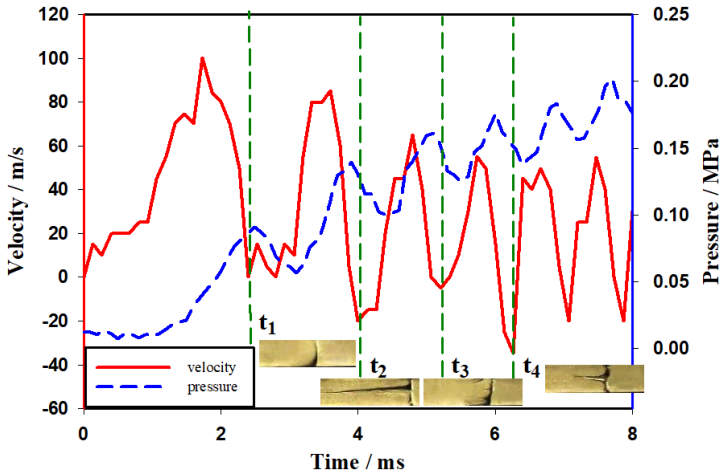


Figure 3. The flame tip velocity of hydrogen-air premixed flame with equivalence ratio=1 in channel (a) (t1: the first flat flame, t2: the first "T-shaped flame", t3: the second flat flame, t4: the distorted tulip flame)

The pressure profile during the propagation of premixed flame in channel (a) is also shown in Fig.3. The pressure was approximately constant before t=1.1 ms which was the time that the flame front first touched the sidewall. The first peak occurred at t=2.5 ms. The increment was about 0.079 MPa. The first minimum value of pressure appeared at about t=3.1ms corresponding to the time of classic tulip flame formation. The subsequent increase of pressure after t=3.1 ms may be ascribed to the pressure wave generated by the cusp collapse. As the flame structure turned to be the "T-shaped flame", the pressure achieved its second maximum value. The "T-shaped flame" presented the same dynamics feature as the first flat flame front. After the "T-shaped flame", the flame lips coalesced. The flame shape transformed to another finger-shaped flame. As the second finger-shaped flame propagated forward, the pressure wave may be produced by the interaction of the flame front and sidewall again. The flame went through the second flat flame and the pressure reached another peak. The flame changed from the second tulip flame to the distorted tulip flame with the pressure changing from the minimal value to the maximal value.

The pressure variation on the PCB sensor was actually determined by its surrounding unburnt gas. The pressure drops in Fig.3 infer that there were reverse flows (from right to left) of unburnt gas, which were probably driven by flame and pressure waves.

To compare the different flame dynamics in the channels of different aspect ratio, the flame tip velocity and pressure in channel (b) was explored as well. Figure 4 shows the flame propagation velocity and pressure in channel (b). The velocity underwent a similar changing pattern as that in Channel (a). The velocity fluctuated but the maximum value decreased with time after the first peak at around t=4.489 ms, which was later than that in channel (a). Although the frequency of velocity fluctuation was smaller in Channel (b), which is in line with the less change in flame shape observed. However, the maximum value of the velocity was larger in channel (b) than that in channel (a).

The pressure of the hydrogen/air premixed flame propagated in channel (b) is shown in Fig.4. The pressure was also constant until the flame front touched the sidewall. Then it increased rapidly. After the classic tulip flame formed, the acceleration of the pressure decreased. The pressure evolution curve presented a more stable shape, but the increment of the pressure was larger

comparing with channel (a).

Compared to Fig.3, there was not any obvious pressure drop during the combustion, which indicates the absence of reverse flow in unburned gas near the sensor.

The maximum pressures in Fig.3 and 4 are not the final pressure build-ups in the channel. The pressure curves are corresponding to the flame shape changes in Fig.1 and 2. Near the end of combustion, the flame was strongly influenced by the end wall, which was neglected in the analyses.

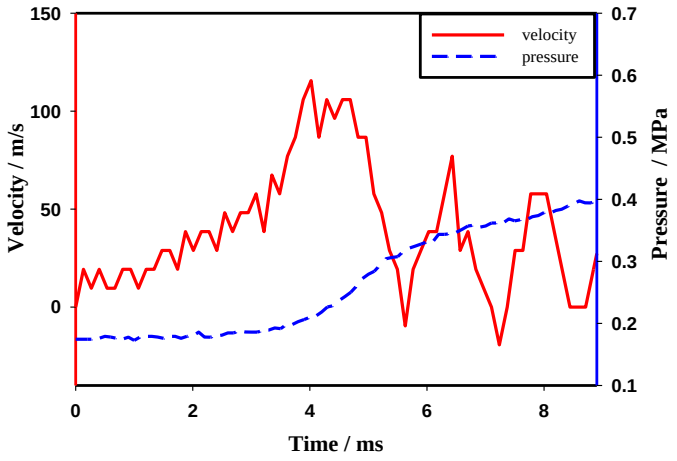


Figure 4. The flame propagation velocity and pressure in channel (b)

### 3.3 Model prediction

In 2007, Bychkov et al. [20] proposed an analytical theory to describe the acceleration process of flame propagating in half-open channels. Thus, the characteristic times mentioned above, i.e. $t_{sphere}$, twall, $t_{tulip}$ , $t_{inv}= t_{tulip} - t_{wall}$ can be predicted. In the theory, all the time are reduced by $R/U_f$, R is the half width of the duct, $U_f$ is the laminar flame speed. The comparisons between the experiment and theory are summarized in Table 1.

Table 1. Comparisons on the characteristic times of the experimental and the theory.

| Reduced characteristic time | Channel (a) (aspect ratio = 12) | Channel (b) (aspect ratio = 6.625) | Analytical theory |
|---|---|---|---|
| $\tau_{sphere}$ | 0.0797 | 0.0744 | 0.0788 |
| $\tau_{wall}$ | 0.2049 | 0.2595 | 0.2549 |
| $\tau_{tulip}$ | 0.4212 | 0.3342 | 0.3337 |
| $\tau_{inv}$ | 0.2163 | 0.0747 | 0.0788 |

The reduced times of flame propagating in channel (b) showed in Table 1 presented a good agreement with that of analytical theory, but the reduced characteristic times in channel (a) showed large difference after spherical expansion. It indicates that, Bychkov's analytical theory [20] cannot predict the acceleration process well in the channel with small width due to the stronger boundary layer effect which is ignored in the theory.

### 3.4 Role of the pressure wave

Pressure wave can be generated in many situations such as the flame front touching the sidewall and tulip flame collapsing [18]. The pressure wave has obvious effect on the flame shape evolution

and flame dynamics observed in this study.

Figure 5 shows the propagation velocity of the flame tip and the pressure growth rate as the function of time in channel (a). In this picture, the velocity and pressure growth rate present a similar tendency during the propagation of flame. Before the initiation of the tulip flame at t=2.4 ms, both the velocity and pressure growth rate suddenly decreased. At the early stage of the flame propagation, the change of velocity and pressure growth rate was approximately synchronous, but the pressure growth rate had a small phase delay which may be attributed to the distance between generation place of pressure wave and the pressure sensor which was placed 6mm away from the right end. The peak of the pressure growth rate can be regarded as the symbol of pressure wave arriving at the pressure sensor. It is proposed that the inflection point of velocity (about t=1.2 ms) is the time when flame front first touched the sidewall. At that time, pressure wave was generated. However, the peak of the pressure growth rate was at about t=1.9 ms. This time lag was treated as the time that the pressure wave took to propagate to the pressure sensor placed 6 mm away from the right end of the channel. A simple calculation was used to testify this assumption. The traveling distance from flame front-right end wall-pressure sensor was about 0.27 m. The sound speed was regarded as 408 m/s in unburnt gas in experimental condition. The time lag that the pressure wave took to propagate to the sensor can be calculated as 0.662 ms, which is close to the interval (about 0.7 ms) between the inflection point of velocity and the peak of pressure growth rate. Based on the flame imaging, the inflection point of the flame velocity could be regarded as the time point of the flame touching the wall.

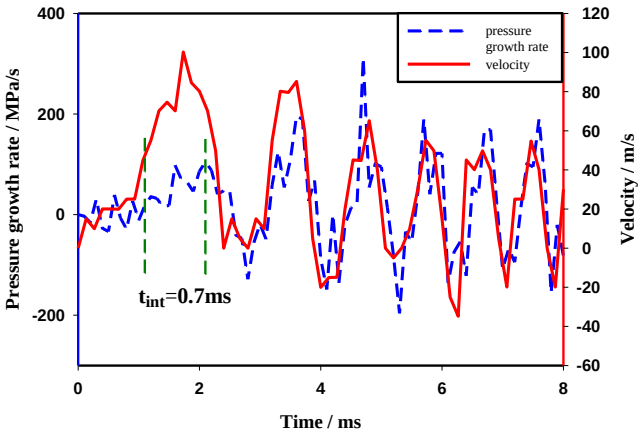


Figure 5. The propagation velocity of flame tip and the pressure growth rate as the function of time in channel (a) (tint is the time interval between the inflection point of velocity and peak of pressure growth rate)

After the pressure wave was reflected and went through the pressure sensor, it continued to propagate. By calculation, at about t=2.533 ms, the reflected pressure wave met with the flame front. But at that moment, the tulip inversion has been started for a while indicating that the pressure wave is not the direct cause of the formation of tulip flame. However, the subsequent remarkable elongation of tulip shape from t=3.067 ms is probably initiated by the pressure wave.

## 4.0 CONCLUSIONS

Combustion and explosions in confined spaces, e.g. chambers, channels, corridors, pipelines, or underground galleries, are key safety problems related to hydrogen energy. Two channels with different aspect ratios were used in present study to simulate the confined spaces. The hydrogen/air premixed flame propagation were observed experimentally in channels to reveal the flame regimes.

First of all, it was found that the flame tip velocity and pressure changed more gently in channels with smaller aspect ratio.

The data gained from our experiments were compared with Bychkov's analytical theory [20]. The flame acceleration process in the channel with larger aspect ratio differed much from the analytical theory, especially after the spherical flame expansion. This can be ascribed to the larger boundary layer effect and acoustic effect in the narrower channel.

The pressure wave is not the main cause of classic tulip inversion. However, the pressure wave may post influence on further flame shape evolutions after classic tulip shape.

In future work, other channels with different aspect ratios will be used. CFD model will be constructed to scrutinize the reveal the physical and chemical mechanisms, which will definitely give a comprehensive view on the effect of channel structure.

## 5.0 ACKNOWLEDGMENT

This work was supported by National Natural Science Foundation of China (Grant No. 51604121); Shanghai Sailing Program (Grant No. 16YF1402000). The authors sincerely thank these supports.

## REFERENCES

1. Bao, C.,Ouyang, M. and Yi, B., Modeling and control of air stream and hydrogen flow with recirculation in a PEM fuel cell system—I. Control-oriented modeling, *International Journal of Hydrogen Energy*, **31**, No. 13, 2006, pp. 1879-1896
2. Dincer, I. and Acar, C., Review and evaluation of hydrogen production methods for better sustainability, *International Journal of Hydrogen Energy*, **40**, No. 34, 2015, pp. 11094-11111.
3. Mallard, E. and Le Chatelier, H., Combustion of explosive gas mixtures, *Ann. mines*, **8**, 1883, pp. 274.
4. Ellis, O. d. C., Flame movement in gaseous explosive mixtures, *J. Fuel Sci.*, **7**, 1928, pp. 502-508.
5. Salamandra, G.,Bazhenova, T. and Naboko, I., Seventh Symposium (International) on Combustion, *Butterworth and Company, Ltd., London*, The Combustion Inst., 1959, pp. 321.
6. Clanet, C. and Searby, G., On the "tulip flame" phenomenon, *Combustion and Flame*, **105**, No. 1-2, 1996, pp. 225-238.
7. Markstein, G., Nonsteady Flame Propagation. 1964, Pergamon Press, Oxford.
8. Starke, R. and Roth, P., An experimental investigation of flame behavior during cylindrical vessel explosions, *Combustion and Flame*, **66**, No. 3, 1986, pp. 249-259.
9. Pocheau, A. and Kwon, C. W., Proceedings of A.R.C. Colloquium, C.N.R.S.-P.I.R.S.E.M., Paris, 1989, pp. 62.
10. Xiao, H.,Wang, Q.,He, X.,Sun, J. and Yao, L., Experimental and numerical study on premixed hydrogen/air flame propagation in a horizontal rectangular closed duct, *International Journal of Hydrogen Energy*, **35**, No. 3, 2010, pp. 1367-1376.
11. Dunn-Rankin, D. and Sawyer, R., Tulip flames: changes in shape of premixed flames propagating in closed tubes, *Experiments in fluids*, **24**, No. 2, 1998, pp. 130-140.
12. Xiao, H.,Wang, Q.,He, X.,Sun, J. and Shen, X., Experimental study on the behaviors and shape changes of premixed hydrogen–air flames propagating in horizontal duct, *International Journal of Hydrogen Energy*, **36**, No. 10, 2011, pp. 6325-6336.
13. Ponizy, B.,Claverie, A. and Veyssière, B., Tulip flame - the mechanism of flame front inversion, *Combustion and Flame*, **161**, No. 12, 2014, pp. 3051-3062.
14. Chen, P.,Li, Y.,Guo, S. and Ji, J., Experimental and numerical study of premixed methane/air flame propagating in various L/D closed ducts, *Process Safety Progress*, **35**, No. 2, 2016, pp. 185-191.
15. Yu, M.,Zheng, K.,Zheng, L.,Chu, T. and Guo, P., Scale effects on premixed flame propagation of hydrogen/methane deflagration, *International Journal of Hydrogen Energy*, **40**, No. 38, 2015, pp. 13121-13133.
16. Xiao, H.,Duan, Q. and Sun, J., Premixed flame propagation in hydrogen explosions, *Renewable and Sustainable Energy Reviews*, **81**, 2018, pp. 1988-2001.
17. Shen, X.,He, X. and Sun, J., A comparative study on premixed hydrogen–air and propane–air flame propagations with tulip distortion in a closed duct, *Fuel*, **161**, 2015, pp. 248-253; (b)
18. Xiao, H.,Houim, R. W. and Oran, E. S., Formation and evolution of distorted tulip flames, *Combustion and Flame*, **162**, No. 11, 2015, pp. 4084-4101

19. Xiao, H.,Houim, R. W. and Oran, E. S., Effects of pressure waves on the stability of flames propagating in tubes, *Proceedings of the Combustion Institute*, **36**, No. 1, 2017, pp. 1577-1583.
20. Bychkov, V.,Akkerman, V. y.,Fru, G.,Petchenko, A. and Eriksson, L.-E., Flame acceleration in the early stages of burning in tubes, *Combustion and Flame*, **150**, No. 4, 2007, pp. 263-276.